

SAN099-0707J
version marked
2/17/99

Note: This is a preprint of a paper being submitted for publication. Contents of this paper should not be quoted nor referred to without permission of the author(s).

To be submitted to Journal of Applied Physics.

RECEIVED
APR 07 1999
OSTI

Effects of Hydrogen in the Annealing Environment On Photoluminescence from Si Nanoparticles in SiO₂

S. P. Withrow, C. W. White, A. Meldrum, and J. D. Budai
Oak Ridge National Laboratory
Oak Ridge, Tennessee

D. M. Hembree, Jr.
Oak Ridge Y-12 Plant
Oak Ridge, Tennessee

and

J. C. Barbour
Sandia National Laboratories
Albuquerque, New Mexico

"The submitted manuscript has been authored by a contractor of the U.S. Government under contract No. DE-AC05-96OR22464. Accordingly, the U.S. Government retains a nonexclusive, royalty-free license to publish or reproduce the published form of this contribution, or allow others to do so, for U.S. Government purposes."

Prepared by the
Oak Ridge National Laboratory
Oak Ridge, Tennessee 37831
managed by
LOCKHEED MARTIN ENERGY SYSTEMS, INC.
for the
U.S. DEPARTMENT OF ENERGY
under contract DE-AC05-96OR22460

February 1999

Sandia is a multiprogram laboratory operated by Sandia Corporation, a Lockheed Martin Company, for the United States Department of Energy under contract DE-AC04-94AL85000.

DISCLAIMER

This report was prepared as an account of work sponsored by an agency of the United States Government. Neither the United States Government nor any agency thereof, nor any of their employees, make any warranty, express or implied, or assumes any legal liability or responsibility for the accuracy, completeness, or usefulness of any information, apparatus, product, or process disclosed, or represents that its use would not infringe privately owned rights. Reference herein to any specific commercial product, process, or service by trade name, trademark, manufacturer, or otherwise does not necessarily constitute or imply its endorsement, recommendation, or favoring by the United States Government or any agency thereof. The views and opinions of authors expressed herein do not necessarily state or reflect those of the United States Government or any agency thereof.

DISCLAIMER

Portions of this document may be illegible in electronic image products. Images are produced from the best available original document.

Effects of Hydrogen in the Annealing Environment on Photoluminescence from Si Nanoparticles in SiO₂

S. P. Withrow, C. W. White, A. Meldrum, and J. D. Budai
Oak Ridge National Laboratory, Oak Ridge, TN 37831

D. M. Hembree, Jr.
Oak Ridge Y-12 Plant, Oak Ridge, TN 37831
and

J. C. Barbour
Sandia National Laboratories, Albuquerque, NM

Abstract

The role of hydrogen in enhancing the photoluminescence (PL) yield observed from Si nanocrystals embedded in SiO₂ has been studied. SiO₂ thermal oxides and bulk fused silica samples have been implanted with Si and subsequently annealed in various ambients including hydrogen or deuterium forming gases (Ar+4%H₂ or Ar+4%D₂) or pure Ar. Results are presented for annealing at temperatures between 200° and 1100°C. Depth and concentration profiles of H and D at various stages of processing have been measured using elastic recoil detection. Hydrogen or deuterium is observed in the bulk after annealing in forming gas but not after high temperature (1100°C) anneals in Ar. The presence of hydrogen dramatically increases the broad PL band centered in the near-infrared after annealing at 1100°C but has almost no effect on the PL spectral distribution. Hydrogen is found to selectively trap in the region where Si nanocrystals are formed, consistent with a model of H passivating surface states at the Si/SiO₂ interface that leads to enhanced PL. The thermal stability of the trapped H and the PL yield observed after a high temperature anneal have been studied. The hydrogen concentration and PL yield are unchanged for subsequent anneals up to 400°C. However, above 400°C the PL decreases and a more complicated H chemistry is evident. Similar concentrations of H or D are trapped after annealing in H₂ or D₂ forming gas; however, no differences in the PL yield or spectral distribution are observed, indicating that the electronic transitions resulting in luminescence are not dependent on the mass of the hydrogen species.

Introduction

Significant effort has been focused in recent years on the formation and characterization of Si nanocrystals. This interest originated with the observation of room temperature photoluminescence (PL) from porous silicon¹ and the interpretation of the light emission in terms of quantum confinement of carriers in nanocrystalline-sized Si structures. In subsequent studies PL has been observed from nanometer-sized crystalline Si particles fabricated using a variety of techniques, including deposition onto substrates by gas phase synthesis or decomposition of silane by plasmas or lasers. Another process that has been widely used for Si nanocrystal formation involves ion implantation of Si into SiO₂ followed by thermal annealing.²⁻¹² At sufficiently high temperatures the implanted excess Si precipitates out from the SiO₂ resulting in embedded Si particles. This approach to synthesis appears well-suited for optoelectronic device applications since the particles formed are in a mechanically robust and chemically stable matrix, the technique allows for some control over nanocrystal size and distribution via processing conditions, and the procedure could be integrated into standard device technologies. Light emitting devices based on nanocrystalline Si would have potential applications in advanced microelectronics. Other applications, including memory structures utilizing charged Si nanocrystals,¹³ have also been proposed.

While photoluminescence has been observed from samples utilizing ion implantation of Si into SiO₂ to form nanocrystals, the origin of the light emission is still being debated. The phenomenon has been attributed to quantum confinement effects by some authors, but it is difficult to reconcile all the data to this model.¹⁴ Other mechanisms, including states at the nanocrystal-Si/SiO₂ interface and/or processing-induced defects, may also play a significant role in the emission. One of the parameters that affects the photoluminescence is the presence of hydrogen. A number of authors have studied the effects hydrogen has on the PL observed from Si nanocrystals in SiO₂. Min et al.⁴ reported that implanting deuterium following ion beam synthesis of Si nanocrystals in SiO₂ quenches luminescence related to defects in the matrix. Subsequent annealing at 500°C in vacuum resulted in a large increase (up to 10-fold) in PL related to the nanocrystals which they attributed to mobility of D in the substrate

and trapping at dangling bonds at the SiO₂/Si interface. Neufeld et al.³ observed that annealing Si-implanted SiO₂ in a rapid thermal annealing furnace in a H₂/N₂ ambient increased the PL by a factor of 3 over a vacuum anneal and attributed this reversible change to the passivation of non-radiative defects by hydrogen. To date, however, no direct measurement of the hydrogen concentration in luminescent samples has been reported.

In the present work, a systematic study of the effects of hydrogen on the PL from Si nanocrystals in SiO₂ is presented. Hydrogen concentrations and depth profiles have been measured in SiO₂ containing Si nanocrystals and correlated with photoluminescence spectra. While luminescence is seen in samples where no H is measured, the presence of H dramatically increases the PL yield but has almost no effect on the PL spectral distribution. In addition, the H selectively traps in the region of the Si nanocrystals at a concentration that is consistent with interface passivation. No hydrogen isotope effects are seen.

Experiment

Si ions were implanted at room temperature into thermal oxide films grown on Si(100) wafers or into bulk fused silica (Corning 7940 glass) substrates. Ion energies between 100 and 400 keV and doses from $1-6 \times 10^{17}$ /cm² were utilized to produce peak excess Si concentrations of $0.5-2 \times 10^{22}$ /cm³. Uniform excess Si concentrations of up to 2×10^{22} /cm³ were produced in several samples by multiple energy implantations. The implanted samples were subsequently furnace annealed at 1100°C for 1 hour to precipitate Si into nanoparticles. Annealing was carried out in several different atmospheres, including flowing Ar+4%H₂ forming gas, Ar+4%D₂ forming gas, or an Ar-only ambient. Samples were removed from the furnace but remained in the ambient to cool radiatively (to <700°C in ~20 s). Alternately, a few samples were held in the furnace and cooled slowly to room temperature over several hours. Selected samples were annealed a second time at various temperatures up to 1100°C.

The presence of Si nanocrystals was directly observed using transmission electron microscopy and x-ray diffraction. Photoluminescence spectra were obtained at room temperature with a double pass spectrometer using the 514-nm line from an Ar ion laser for excitation and a photomultiplier for detection. Concentration profiles of H in the oxides were measured using elastic recoil detection (ERD) of a 24 MeV Si^{+5} ion beam incident at 75 degrees from the surface normal. Recoiled H was detected at a forward scattering angle of 30 degrees in a surface barrier detector behind a 12-micron mylar foil. The experimental geometry was calibrated, just before data collection from the SiO_2 samples, using a 300 nm thick Si_3N_4 standard sample with a uniform concentration depth profile of 6 at.% H. Depths down to ~800 nm in the SiO_2 could be probed using the ERD technique with a depth resolution of 30-50 nm. D was depth profiled in selected samples using the same technique.

Results

If Si-implanted SiO_2 is annealed at 1100 °C, then precipitation of the excess Si occurs. The transmission electron microscopy (TEM) images shown in Figure 1 confirm the formation of nanocrystals in the Si-implanted SiO_2 wafers. For a uniform excess Si concentration of 5×10^{21} ions/cm³ achieved by multiple energy implants, separate and well-defined regions of dark contrast having an average diameter of approximately 3 nm are readily visible using slightly defocused imaging conditions (Fig. 1a). Continuous lattice fringes were not observed; however, these regions of dark contrast did not occur in the unimplanted portion of the specimen. The dark contrast areas are, therefore, tentatively identified as silicon-rich clusters. In a sample with a uniform excess Si concentration of 2×10^{22} ions/cm³, relatively large (> 5 nm), well-defined nanocrystals were observed (Fig. 1b). The distribution of nanocrystal sizes is relatively broad in this sample. An additional specimen implanted with a single ion energy (400 keV, 1.5×10^{17} ions/cm³) also showed a broad distribution of nanocrystal sizes after annealing at 1100°C. The largest particles were located at a region corresponding the peak concentration of implanted Si, and the smaller particles were located at the tails

of the implant distribution. The average size of the Si precipitates is, therefore, largely dependent on the concentration of implanted silicon.

Figure 2 shows PL spectra obtained from fused silica implanted with 400 keV Si to a dose of 1.5×10^{17} Si/cm². The PL from the as-implanted sample peaks at 650 nm and arises from defects introduced into the matrix during implantation.⁷ Annealing at 950°C greatly reduces this defect luminescence and may induce formation of small nanoparticles. After annealing at 1100°C, Si nanoparticles are visible in TEM and an intense PL band peaked at ~750 nm is observed.

Figure 3 shows PL spectra from fused silica implanted with Si (200 keV, 1.0×10^{17} /cm², RT) and then annealed for 1 h at 1100°C in three different environments. A broad peak centered at just less than 750 nm is observed when the ambient is flowing Ar+4%H₂. A spectrum with the same intensity and spectral distribution is obtained when the 4% hydrogen is replaced with 4% deuterium (dashed curve). A sample annealed in an Ar ambient at the same temperature and for the same length of time has a PL yield lower by a factor of approximately four. Hence the intensity of the PL is strongly dependent on the presence of hydrogen in the annealing environment. However, the spectral distribution is the same as annealing in Ar+4%H₂.

Results similar to those in Fig. 3 are observed for Si nanocrystals formed in a thermal oxide on Si. For the latter substrates, however, PL yields are typically higher by 30 to 50%. The source of this increased PL may be related to partial reflection of the incident laser light from the SiO₂/Si interface, resulting in increased excitation. Interference effects in the PL spectrum due to reflection of the excitation light at an interface was previously observed to cause resonant PL results seen for Ge nanoparticles in thermal SiO₂ layers.¹⁵

For the sample in Fig. 3 that was annealed in Ar, a subsequent 1100°C anneal in Ar+4%H₂ results in an increase in PL to nearly the same yield obtained for the Ar+4%H₂ anneal. By alternating between

Ar and forming gas anneals the PL can be cycled between higher and lower yields, indicating that the hydrogen effect is reversible. It should be noted, however, that it is not possible to reproduce the same yields indefinitely by cycling since the PL yield is also a function of annealing time. For a uniform implantation of $5 \times 10^{21} / \text{cm}^3$ the PL reaches a maximum after annealing for 1 h at 1100°C in hydrogen forming gas. Annealing this sample for 24 h at 1100°C results in a reduction in PL yield of more than 80%. This decrease is believed due to Ostwald ripening of the nanoparticles coupled with an inverse size-dependence for luminescence. A PL dependence on annealing time has previously been reported.⁷

The spectra presented in Fig. 3 show that the annealing ambient has a strong effect on the PL yield. In particular, the presence of H_2 (or D_2) in the ambient leads to an increased PL over that observed after annealing in only Ar. To understand these results, profiles of hydrogen in the surface layer of the oxide after different processing conditions have been obtained using elastic recoil detection. The hydrogen distribution in a thermal oxide implanted with Si (200 keV, $1 \times 10^{17} / \text{cm}^2$, RT) is given by the dotted curve in Fig. 4. The large peak at the surface is attributed to adsorbed H or surface contamination such as water or hydrocarbons. This peak is commonly observed for unannealed SiO_2 or SiO_2/Si samples. The bulk H concentration in this as-implanted sample, ~ 0.06 at. %, is uniform with depth down to 800 nm, which is the depth that the ERD technique can probe in these samples without interference from an oxygen signal. The same level and distribution of H was measured in the unimplanted thermal oxide indicating implantation does not affect the H concentration. The noise levels in the spectra are ± 0.02 at. %. A similar uniform H profile, but at twice the H concentration, has been measured in an unimplanted fused silica sample, indicating that the amount of H incorporated into the oxide varies with the SiO_2 preparation technique. Also shown in Fig. 4 for comparison are spectra obtained after annealing at 1100°C for 1 h either in $\text{Ar}+4\%\text{H}_2$ (solid curve) or only Ar (dashed curve). Each of these spectra shows a decrease in the surface H concentration by roughly a factor of four, consistent with the high temperature anneal driving off surface contaminants. For the Ar-only annealed sample no detectable bulk H remains, indicating the uniform H concentration observed in the

sample before annealing has diffused out of the region probed as a result of the 1100°C anneal. In contrast, when a sample is heated to the same temperature, 1100°C, and subsequently cooled with H₂ in the ambient, then H is observed in the bulk. However, the H is no longer distributed throughout the sample, as was the case before annealing, but is now limited to a profile with a peak at a depth of ~300 nm with a distribution that can be reasonably fit with a Gaussian. No H is detectable deeper than roughly 700 nm.

The PL yields and the retained hydrogen profiles given in Figs. 3 and 4 were all obtained following 1100°C anneals. Additional information about the effect of H on PL in these samples was obtained using subsequent lower temperature anneals. Thermal oxide samples were processed in hydrogen forming gas under conditions that produce the higher PL yield seen in Fig. 3 (1 h at 1100°C) and then annealed a second time for 1 h in Ar-only at selected temperatures between 200 and 1100°C. In Fig. 5 are plotted the maximum in the PL yield from these twice-annealed samples (open circles) and also the peak retained H (open squares) as a function of the temperature of the second anneal. Also shown for comparison are the peak yields from Fig. 3 for annealing once at 1100°C for 1 h in Ar+4%H₂ (solid circle) or Ar (triangle). As seen in Fig. 5, for second anneal temperatures up to 400°C there is no effect on the measured PL or retained H relative to one anneal in Ar+4%H₂. However, between 400 and 800°C the PL yield decreases with increasing temperature. A second anneal at 800°C results in the same PL measured from a sample annealed once for 1h in Ar-only. These PL changes above 400°C are accompanied by changes in the H concentration, first an increase between 400 and 600°C and then a decrease at higher temperatures. Both the increase and the decrease are associated with changes in the H chemistry, including detrapping and diffusion. These effects are discussed below. It should be noted that the PL decrease seen in Fig. 5 is not a result of the Ostwald ripening process mentioned above. The PL yield changes only about 10% for anneals between 1 and 2 h at 1100°C in Ar+4%H₂ and would be expected to change even less at lower temperatures.

Elastic recoil detection has also been used to measure the deuterium retained in a thermal oxide following an 1100°C anneal in deuterium forming gas. The spectrum is given in Fig. 6. Except for the ambient gas, the substrate and processing were the same as used for the ERD results in Fig. 4. The deuterium profile is qualitatively the same as for annealing in a hydrogen forming gas, indicating that hydrogen and deuterium behave similarly. No D peak at the surface is seen, evidence that the hydrogen in the surface peak in Fig. 4 is not a result of the annealing. A hydrogen profile was also measured from the sample that underwent a deuterium forming gas anneal. The H in the bulk in the as-implanted sample has been essentially removed as a result of the anneal but a hydrogen peak is seen on the surface. No D is seen in samples annealed in hydrogen forming gas, as expected.

Discussion

Hydrogen is known to exist in silicon dioxide in several chemical states: as interstitial molecular hydrogen H_2 , bonded directly to Si, and as the hydroxyl OH with the OH radicals either interstitial or attached to dangling Si bonds. The amount of hydrogen in the SiO_2 and its chemistry are dependent on the oxide preparation and subsequent processing. The concentration of H observed in the unimplanted oxide samples used here, on the order of 0.1 atomic percent, is consistent with a large body of work reviewed by Revez¹⁴ which reported the presence of 10^{19} - 10^{20} hydrogen species per cm^3 as Si-OH and Si-H groups in steam- and O_2 -grown thermal oxides, respectively. Fused silica is also known to contain similar H amounts.¹⁵ At room temperature hydrogen is stable in the oxide. Fink reported no change in the hydrogen distribution in silica over long times, indicating that detrapping and diffusion are not significant at RT.¹⁶ In contrast, H-containing species are mobile in the lattice at elevated temperatures. For example, OH radicals trapped in the bulk oxide can be released at annealing temperatures $\geq 600^\circ C$.¹⁷ The large open structure of SiO_2 facilitates interstitial diffusion, with the movement affected (hindered) by the equilibrium between the H_2 and OH radical and by trapping and detrapping of the hydrogen species at dangling bond sites. Heating at temperatures sufficiently high that H detraps and/or diffuses leads to changes in the ERD spectra. Although the ERD results

presented here do not distinguish the bonding of the hydrogen, by correlation to PL spectra some interesting conclusions can be drawn about the effects of hydrogen on the luminescence.

Implantation does not change the bulk hydrogen concentration or distribution. While the number of dangling Si bonds in the region of the implant would be expected to increase as a result of implantation damage, H does not diffuse to this region at RT either from the surface or from deeper in the bulk. On the other hand, significant changes in the H profile are induced by thermal processing. Following annealing at 1100°C hydrogen remains in the bulk, but only in the region of the Si implant. No hydrogen is observed in the bulk of an unimplanted sample after an 1100°C, 1 h anneal in hydrogen forming gas (although hydrogen associated with the surface is present for this case). Hence, the Si implant and/or subsequent formation of nanocrystals provides the trapping sites necessary to retain H. In Fig. 7 a TRIM¹⁸ calculation (solid line) of the implant profile for 200 keV Si into SiO₂ is compared to the bulk H concentration (dotted line) from Fig. 4 for an anneal in forming gas. Surface hydrogen in the ERD spectrum has been fit with a Gaussian and subtracted off. The theoretical implant profile peaks at 320 nm which is nearly identical to the broad maximum in the H distribution. This agreement indicates a correlation between the implant and the trapped H. On the other hand, the distribution widths differ, with the TRIM calculation extending down to ~500 nm while the H distribution is broader and measurable down to almost 800 nm. Part of this difference can be attributed to the depth resolution of the ERD measurements, ~50 nm, as can be inferred from the width of the H peak at the surface in Fig. 4. The broader H profile indicates that the amount of H trapped is not proportional to the local excess implant Si concentration. It has been suggested that the H is retained at the SiO₂/Si interface where it passivates dangling bonds.^{3,4} If the amount of H retained is proportional to the surface area of the nanocrystals, the net effect would be to broaden the H distribution relative to the implant concentration. This is because the size of the nanocrystals varies across the implant profile, with the average size related to the implanted concentration. Smaller nanocrystals have a larger surface-to-volume ratio and would trap relatively more H.

It is interesting to consider where the H is located. After annealing, H is selectively seen only in the layer containing Si nanocrystals. That observation, plus the enhancement effect it has on the PL yield, supports the conclusion that H is trapped at the Si/SiO₂ interface. Selective accumulation of D at a SiO₂/Si interface for annealing at temperatures up to 230°C has been previously reported.²⁰ While a direct verification of this hypothesis is not possible here, a comparison between the measured amount of H versus the number of available surface states does suggest it is quantitatively reasonable. The measured peak H concentration of 0.06 at.% occurs at a depth where the excess Si implant concentration is $5 \times 10^{21} / \text{cm}^3$.¹⁹ As seen in Fig. 1a, this excess Si and the annealing conditions used produce precipitates of ~3 nm. If it is assumed that all the implanted Si at the peak of the profile precipitates into 3 nm nanocrystals and that all the measured H is on the nanocrystal interface, the H density would be $2 \times 10^{13} \text{ H/cm}^2$. This H density is somewhat higher than the total interface state density expected at the SiO₂/Si interface.²⁰

Annealing in either hydrogen or deuterium forming gas enhances the PL. While it may not be surprising that both isotopes have a similar effect, it is significant that there is no isotopic effect observed in the PL. Hydrogen and deuterium have an equivalent effect on both the PL yield and spectral distribution. From this latter result it can be concluded that the mechanism responsible for the PL does not involve transition energy levels that are isotope dependent. This result is in contrast to a recent study on the hydrogen isotope effect on luminescence from porous Si. Porous silicon passivated with D has a PL yield significantly blue shifted in comparison to an identical sample passivated with H.²¹ This shift has been explained in terms of energy level differences in isotope-dependent vibrational surface states involved in the radiative transitions. Clearly these results differ markedly from what is found here and suggest that the mechanisms for the PL are different.

The temperature at which H becomes mobile in these samples, >400°C, can be inferred from Fig. 5. Annealing below this temperature causes no changes either in the measured H or in the PL yield. On the other hand, at higher temperatures changes are seen and the relation between the bulk H and PL

becomes more complicated. The small increase in H seen following Ar anneals at 500 and 600°C indicates that hydrogen diffuses into the implanted region at these temperatures either from the surface or possibly from the interface between the oxide and the Si substrate (the only available sources of H). However, the corresponding decrease in PL indicates that in addition to hydrogen diffusing in, the configuration of the bulk hydrogen that enhances PL also undergoes a change. Between 600 and 800°C there is a PL yield decrease as the amount of H trapped decreases. This correlation suggests that as the second anneal temperature is increased in the temperature range between 400 and 800°C, the amount of hydrogen trapped at the interface which affects the PL yield decreases. Johnson et al. observed a release of D at the SiO₂/Si interface for vacuum anneals above 500°C.²⁰ The PL yield is function of the amount of H trapped in a specific bonding configuration at the interface, whereas the H measurement can include other H in the bulk (or at the interface) that does not affect the PL. By 800°C the PL yield has fallen to a level which is observed for an Ar only anneal at 1100°C (for which no H remains as seen in Fig. 4). Hence the H remaining in the sample in Fig. 5 after a second 800°C anneal would appear to have no effect on the PL. It should be noted that the observation of a PL yield in the absence of measurable hydrogen, or when the H is configured such as not to effect the PL, indicates that H is not required to explain the mechanism of luminescence. Radiative recombination can occur without hydrogen passivation. It has been suggested that other species, such as oxygen bonded to the Si at the nanocrystal interface, also may offer some degree of passivation.²² It is important to note that the PL observed in the absence of measurable H has the same spectral distribution as with measureable H. Clearly the mechanism for the PL and the mechanism for H enhancing the PL are independent.

In conclusion, quantitative profiles of hydrogen have been measured in fused silica and thermal SiO₂ layers that have been implanted and annealed to form Si nanocrystals. The hydrogen is selectively trapped in the region of the nanocrystals and enhances the PL yield significantly, supporting a model for PL involving increased radiative emission as a result of hydrogen passivation of defects at the nanocrystal/SiO₂ interface. At annealing temperatures greater than ~400°C the hydrogen is mobile, and at 600°C moves away from the region of the nanocrystals with an accompanying decrease in PL

yield. This suggests a PL yield dependent on the amount of H trapped at the interface, although bulk hydrogen that does not appear to affect the PL yield complicates this observation. Information on the bonding configuration of the H is needed to get a better understanding the hydrogen role. Photoluminescence is observed from samples that have been processed such that no hydrogen is measured using the ERD technique, indicating radiative recombination occurs with no or low levels of hydrogen present. Finally, annealing in either a hydrogen or deuterium forming gas ambient results in equivalent PL yields and spectral distributions which means that the hydrogen species, while enhancing the PL yield, it is not involved directly in the radiative emission mechanism.

Acknowledgements

Oak Ridge National Laboratory is managed by Lockheed Martin Energy Research Corp. for the U.S. Department of Energy under contract number DE-AC05-96OR22464. Sandia is a multiprogram laboratory operated by Sandia Corporation, a Lockheed Martin Company. The work at Sandia was supported by the U.S. DOE Office of Basic Energy Sciences (Division of Materials Sciences/Metals and Ceramics) under contract DE-AC04-94AL85000.

References

1. L. T. Canham, *Appl. Phys. Lett.* **57**, 1046 (1990).
2. C. W. White, J. D. Budai, S. P. Withrow, J. G. Zhu, E. Sonder, R. A. Zuhr, A. Meldrum, D. M. Hembree, Jr., D. O. Henderson, and S. Prawer, *Nucl. Instrum. Methods in Phys. Res. B* **141**, 228 (1998); C. W. White, S. P. Withrow, A. Meldrum, J. D. Budai, D. M. Hembree, J. G. Zhu, D. O. Henderson, and S. Prawer, *Mat. Res. Soc. Proc.*, vol. 507, (1998).
3. E. Neufeld, S. Wang, R. Apetz, Ch. Buchal, R. Carius, C. W. White, and D. K. Thomas, *Thin Solid Films* **294**, 238 (1997).
4. K. S. Min, K. V. Shcheglov, C. M. Yang, Harry A. Atwater, M. L. Brongersma, and A. Polman, *Appl. Phys. Lett.* **69**, 2033 (1996).
5. H. A. Atwater, K. V. Shcheglov, S. S. Wong, K. J. Vahala, R. C. Flagan, M. L. Brongersma, and A. Pohlman, *Mat. Res. Soc. Symp. Proc.* **316**, 409 (1994); M. L. Brongersma, A. Polman, K. S. Min, and H. A. Atwater, *J. Appl. Phys.*, submitted
6. T. Shimizu-Iwayama, S. Nakao, K. Saitoh, and N. Itoh, *J. Phys.: Condensed Matter* **6**, L601 (1994); T. Shimizu-Iwayama, Norihiro Kurumado, David E. Hole, and Peter D. Townsend, *J. Appl. Phys* **83**, 6018 (1998).
7. T. Shimizu-Iwayama, K. Fujita, S. Nakao, K. Saitoh, T. Fujita, and N. Itoh, *J. Appl. Phys.* **75**, 7779 (1994).
8. P. Mutti, G. Ghislotti, S. Bertoni, L. Bonoldi, G. F. Cerofolini, L. Meda, E. Grilli, and M. Guzzi, *Appl. Phys. Lett.* **66**, 851 (1995).
9. T. Komoda, J. P. Kelly, A. Nejim, K. P. Homewood, P. L. F. Hemment, and B. J. Sealy, *Mat. Res. Soc. Symp. Proc.* **358**, 163 (1995).
10. T. Fischer, V. Petrova-Koch, K. Shcheglov, M. S. Brandt, and F. Koch, EMRS Spring Meeting, 1995.

11. L.-S. Liao, X.-M. Bao, X.-Q. Zheng, N.-S. Li, and N.-B. Min, *Appl. Phys. Lett.* **68**, 850 (1996).
12. G. A. Kachurin, K. S. Zhuravlev, N. A. Pazdnikov, A. F. Leier, I. E. Tyschenko, V. A. Volodin, W. Skorupa, and R. A. Yankov, *Nucl. Instrum. Methods in Phys Res. B* **127/128**, 583 (1997).
13. Sandip Tiwari, Farhan Rana, Hussein Hanafi, Allan Hartstein, Emmanuel F. Crabbé, and Kevin Chan, *Appl. Phys. Lett.* **68**, 1377 (1996).
14. G. Revesz, *J. Electrochemical Soc.* **126**, 122 (1979).
15. David L. Griscom, *J. Appl. Phys.* **58**, 2524 (1985).
16. D. Fink, J. Krauser, D. Nagengast, T. Almeida Murphy, J. Erxmeier, L. Palmetshofer, D. Bräunig, and A. Weidinger, *Appl. Phys. A* **61**, 381 (1995).
17. R. A. B. Devine, *J. Appl. Phys.* **56**, 563 (1984).
18. J. F. Ziegler, "Transport of Ions in Matter" (TRIM 98), IBM Corp. Software, (1998); J. F. Ziegler, J. P. Biersack, and U. Littmark, *The Stopping and Range of Ions in Solids*, ed. by J. F. Ziegler (Pergamon Press, New York, 1985) vol. 1.
19. TRIM calculation of the peak concentration corresponding to 200 keV, 1×10^{17} Si/cm².
20. N. M. Johnson, D. K. Biegelsen, and M. D. Moyer, *J. Vac. Sci. Technol.* **19**, 390 (1981).
21. Takahiro Matsumoto, Yasuaki Masumoto, Shinichi Nakashima, and Nobuyoshi Koshida, *Thin Solid Films* **297**, 31 (1997).
22. L. N. Dinh, L. L. Chase, M. Balooch, W. J. Siekhaus, and F. Wooten, *Phys. Rev.* **B54**, 5029 (1996).

Figure Captions

1. Cross-section micrographs showing Si nanocrystals formed in SiO₂ following annealing of uniform excess Si implantation of (a) $5 \times 10^{21}/\text{cm}^3$ and (b) $2 \times 10^{22}/\text{cm}^3$ at 1100°C for 1h in flowing Ar+4%H₂.
2. PL spectra from Si (400 keV, $1.5 \times 10^{17}/\text{cm}^2$, RT) implanted SiO₂ as-implanted and after annealing at 950°C and 1100°C for 1h in Ar+4%H₂.
3. PL spectra from Si nanocrystals formed in fused Si after annealing in either Ar+4%H₂, Ar+4%D₂ (dashed line), or pure Ar.
4. Hydrogen depth profiles from a thermal oxide as-implanted with Si (dashed) and annealed at 1100°C for 1h in Ar+4%H₂ (solid) or in Ar (dotted).
5. Maximum PL yield (open circles) and retained H (open squares) vs. anneal temperature from Si nanocrystals formed in a thermal oxide by annealing in Ar+4%H₂ and subsequently annealed a second time in only Ar. For comparison, the maximum PL yield for a single anneal in either Ar+4%H₂ (filled circle) or Ar (filled triangle) are plotted. The hydrogen yield is normalized to the PL yield for a single anneal in Ar+4%H₂.
6. Deuterium profiles following annealing at 1100°C for 1 h in Ar+4%D₂ or Ar+4%H₂.
7. Comparison of TRIM calculation for Si implantation into SiO₂ (solid line) and the measured bulk H distribution (dotted line) following annealing in Ar+4%H₂ at 1100°C for 1 h.

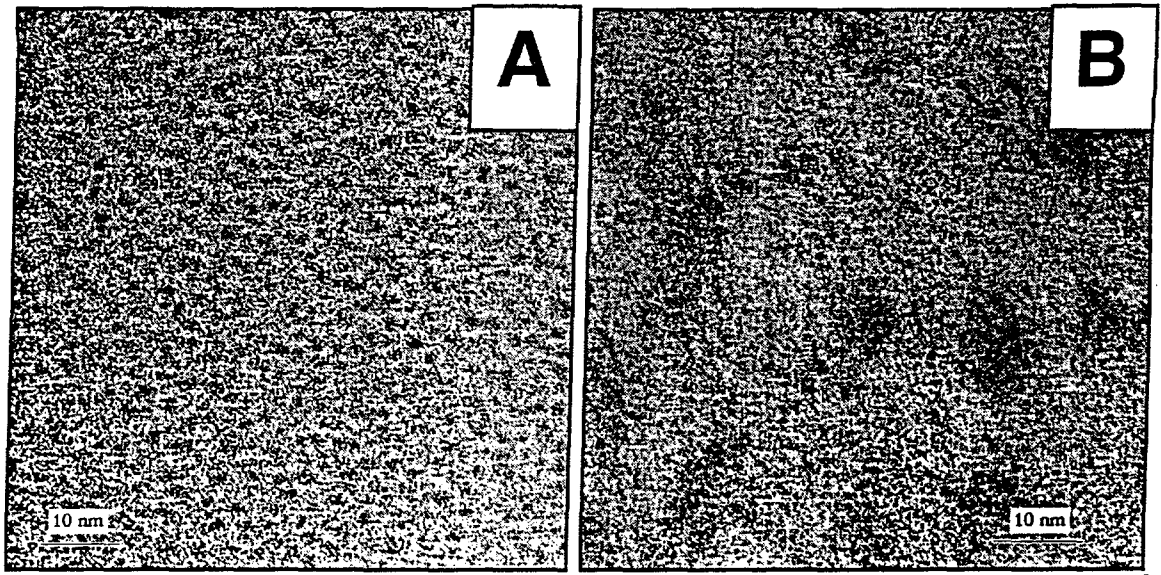


Fig. 1 Cross-section micrographs showing Si nanocrystals formed in SiO₂ following annealing of uniform excess Si implantation of (a) $5 \times 10^{21}/\text{cm}^3$ and (b) $2 \times 10^{22}/\text{cm}^3$ at 1100°C for 1h in flowing Ar+4%H₂.

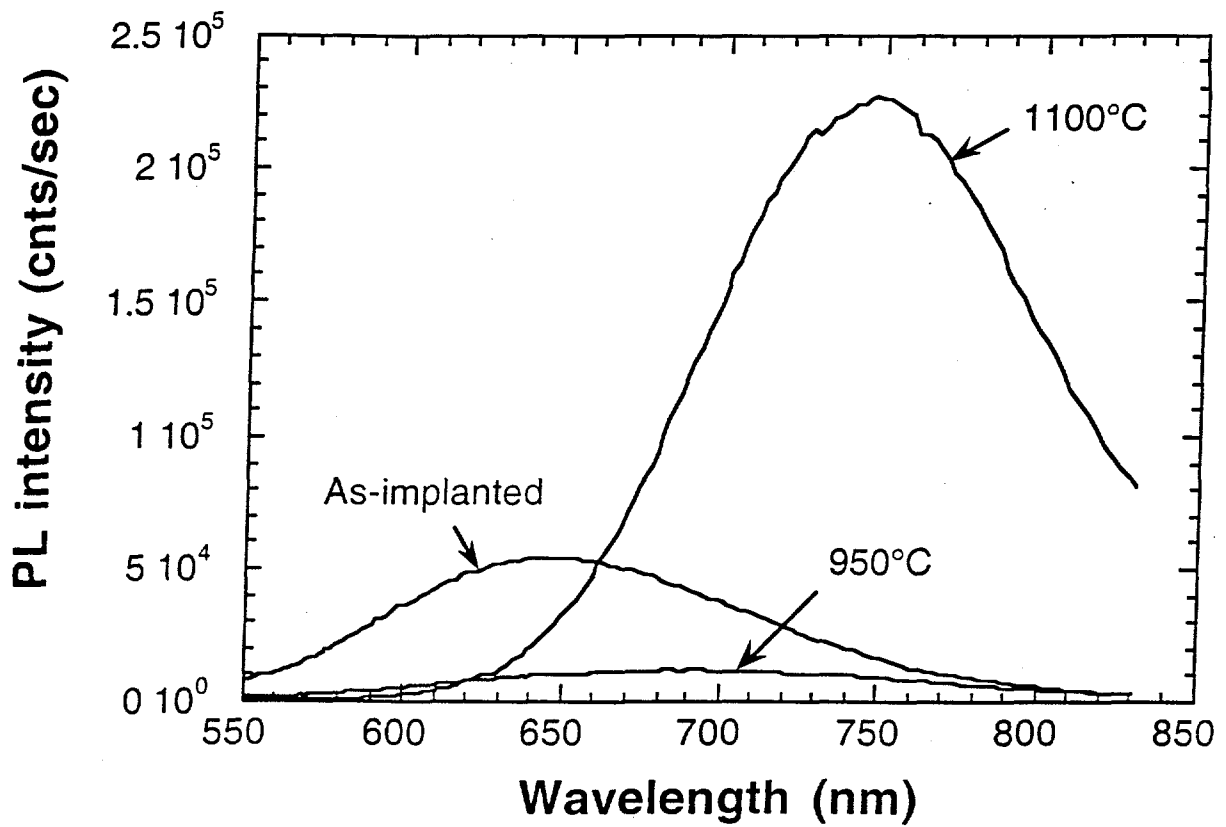


Fig. 2 PL spectra from Si (400 keV, $1.5 \times 10^{17}/\text{cm}^2$, RT) implanted SiO_2 as-implanted and after annealing at 950°C and 1100°C for 1h in Ar+4% H_2 .

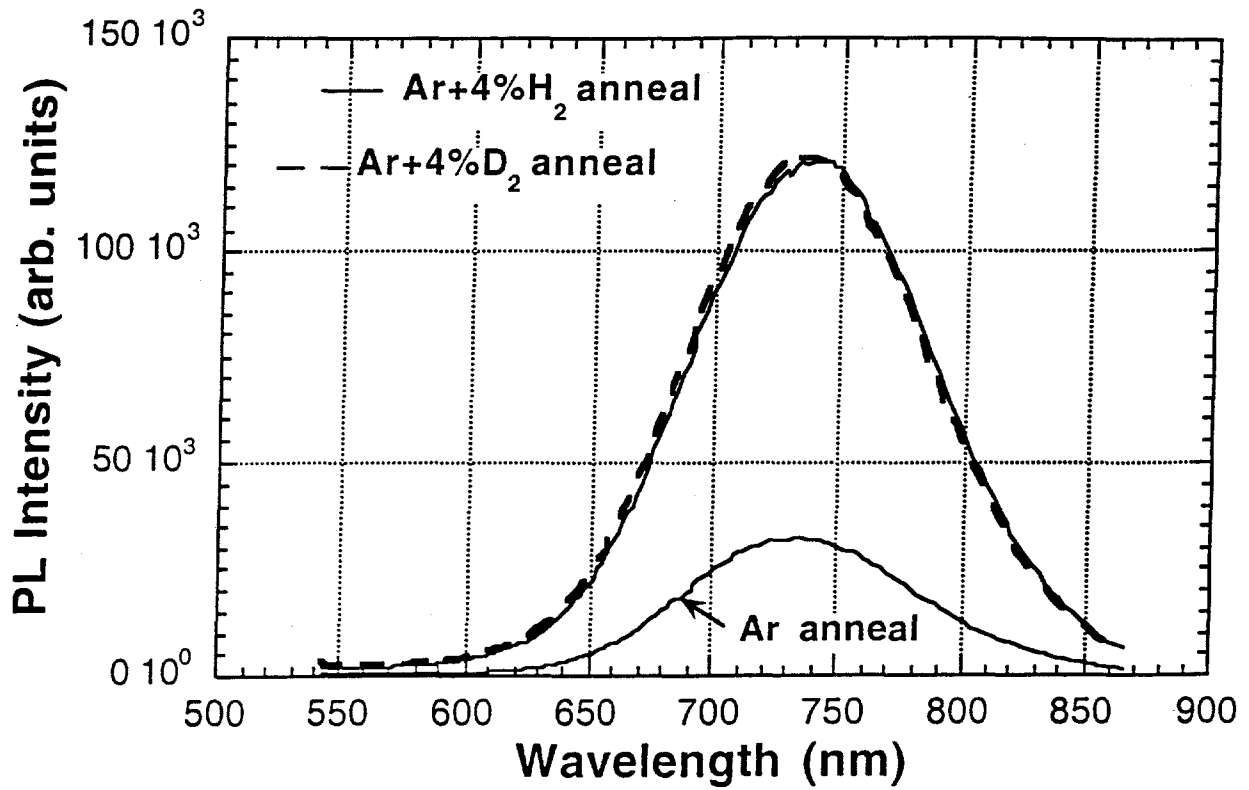


Fig. 3. PL spectra from Si nanocrystals formed in fused Si after annealing in either Ar+4% H_2 , Ar+4% D_2 (dashed line), or pure Ar.

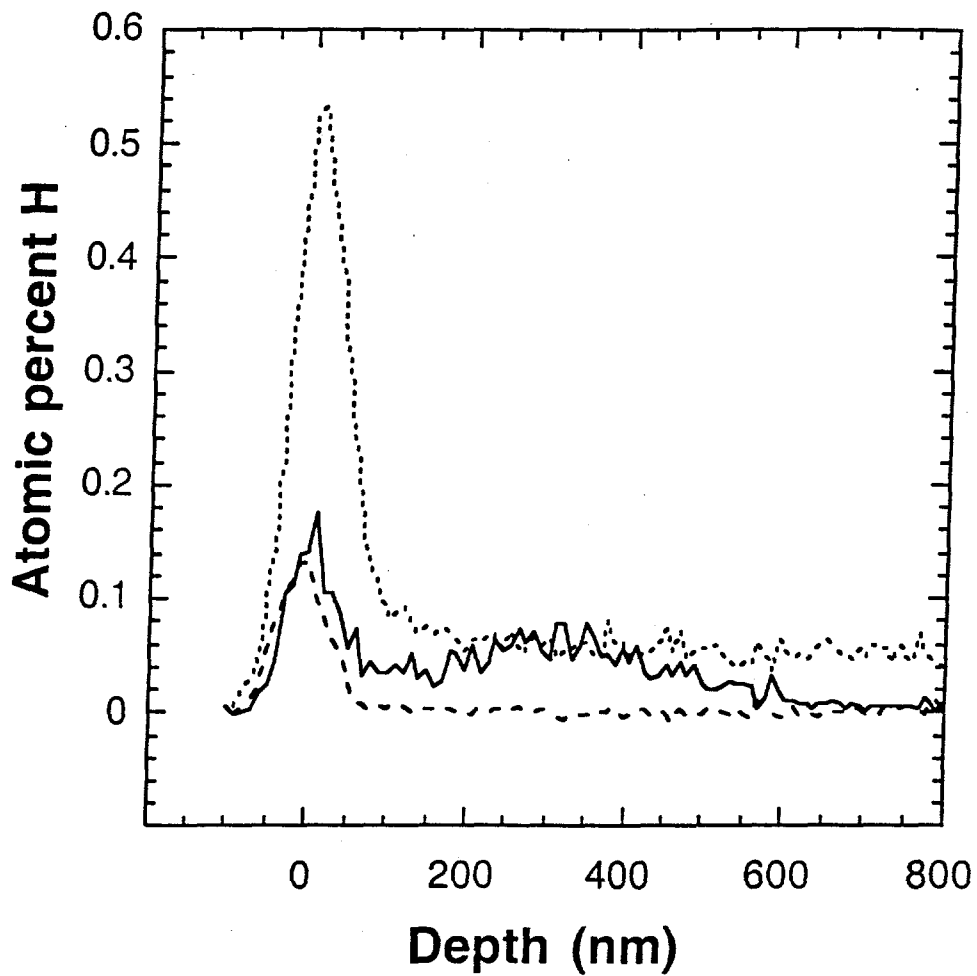
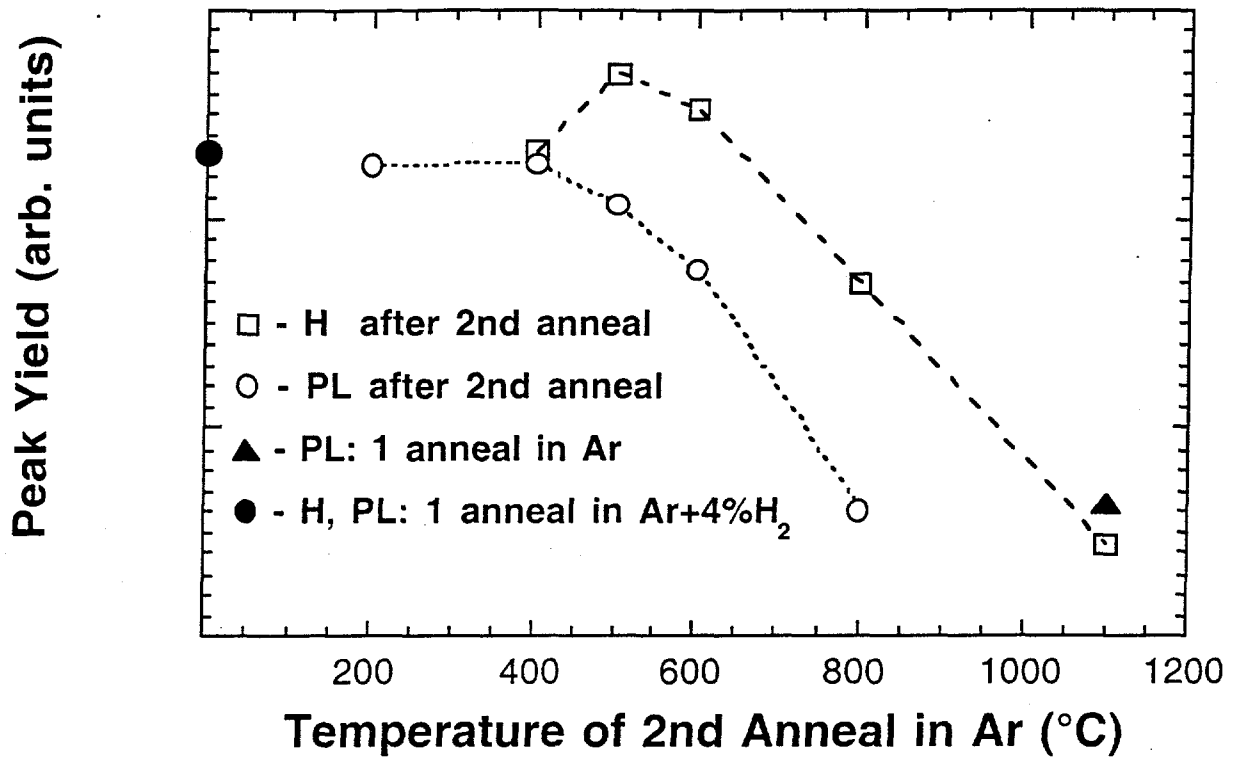


Fig. 4. Hydrogen depth profiles from a thermal oxide as-implanted with Si (dashed) and annealed at 1100°C for 1h in Ar+4%H₂ (solid) or in Ar (dotted).



5. Maximum PL yield (open circles) and retained H (open squares) vs. anneal temperature from Si nanocrystals formed in a thermal oxide by annealing in Ar+4% H_2 and subsequently annealed a second time in only Ar. For comparison, the maximum PL yield for a single anneal in either Ar+4% H_2 (filled circle) or Ar (filled triangle) are plotted. The hydrogen yield is normalized to the PL yield for a single anneal in Ar+4% H_2 .

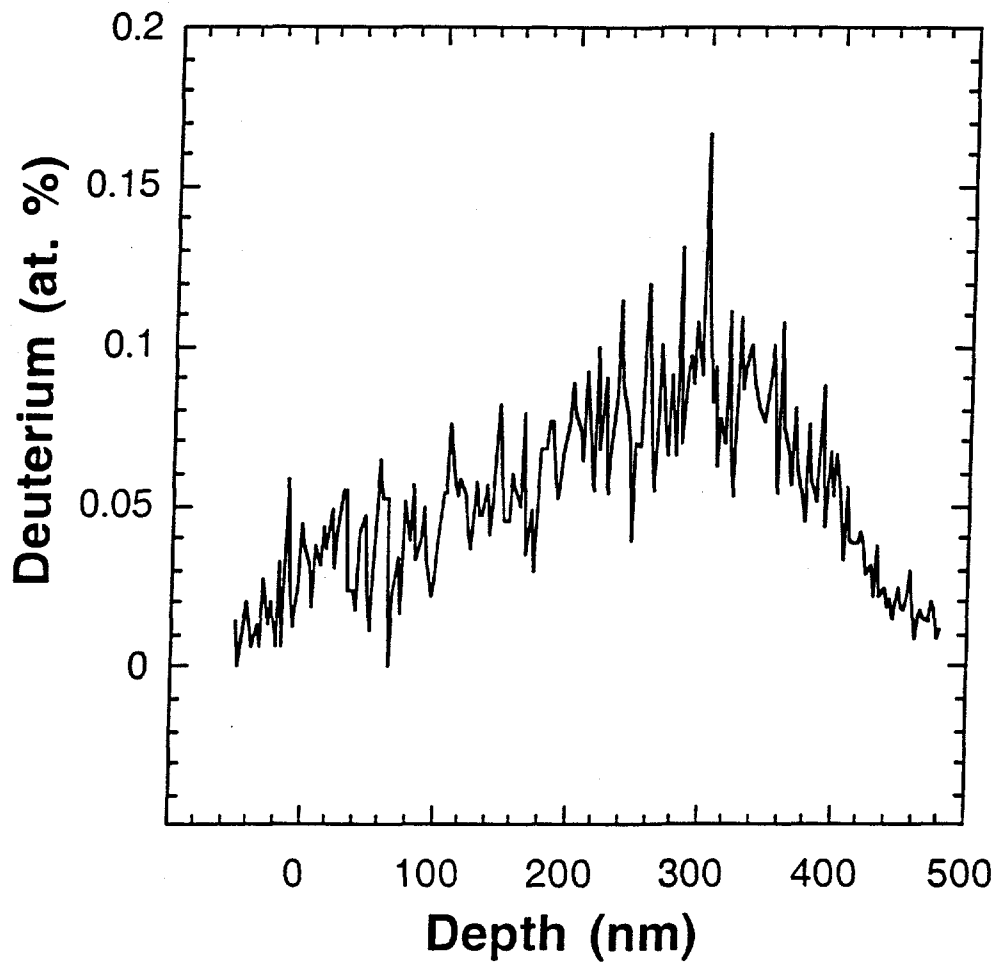


Fig. 6 Deuterium profiles following annealing at 1100°C for 1 h in Ar+4%D₂ or Ar+4%H₂.

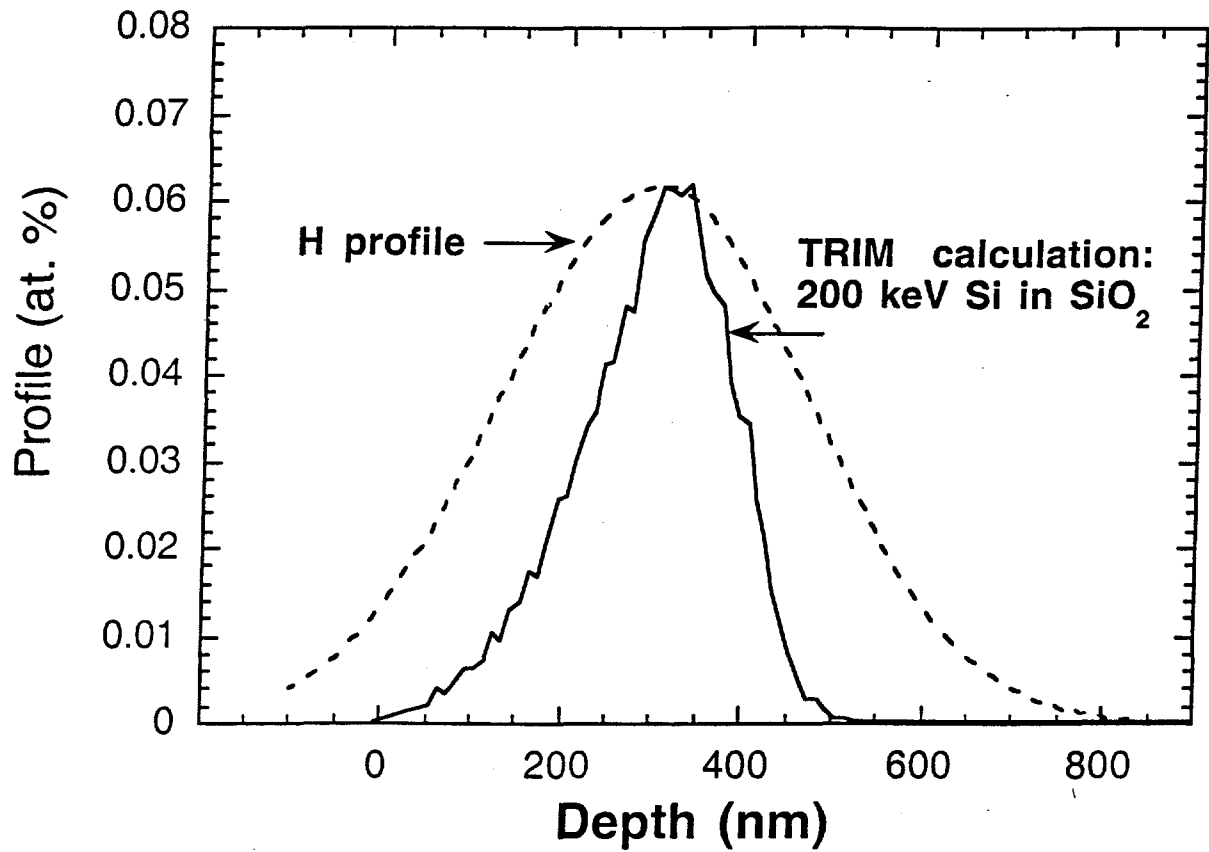


Fig. 7. Comparison of TRIM calculation for Si implantation into SiO₂ (solid line) and the measured bulk H distribution (dotted line) following annealing in Ar+4%H₂ at 1100°C for 1 h.